Autophagy activation promotes clearance of α-synuclein inclusions in fibril-seeded human neural cells

Received for publication, April 3, 2019, and in revised form, July 28, 2019 Published, Papers in Press, August 2, 2019, DOI 10.1074/jbc.RA119.008733

Jianqun Gao[‡§¶1], **Gayathri Perera**[‡], **Megha Bhadbhade**[§], **Glenda M. Halliday**[‡§¶2], **and Nicolas Dzamko**[‡§¶3]

From the [‡]*ForeFront Dementia and Movement Disorders Laboratory, Brain and Mind Centre, Central Clinical School, Faculty of Medicine and Health, University of Sydney, Camperdown, New South Wales 2050, Australia,* [§]*School of Medical Sciences, Faculty of Medicine, University of New South Wales, Kensington, New South Wales 2033, Australia, and* [¶]*Neuroscience Research Australia, Randwick, New South Wales 2031, Australia*

Edited by Paul E. Fraser

There is much interest in delineating the mechanisms by which the α-synuclein protein accumulates in brains of individuals with Parkinson's disease (PD). Preclinical studies with rodent and primate models have indicated that fibrillar forms of α-synuclein can initiate the propagation of endogenous α-synuclein pathology. However, the underlying mechanisms by which α-synuclein fibrils seed pathology remain unclear. To investigate this further, we have used exogenous fibrillar α-synuclein to seed endogenous α-synuclein pathology in human neuronal cell lines, including primary human neurons differentiated from induced pluripotent stem cells. Fluorescence microscopy and immunoblot analyses were used to monitor levels of α-synuclein and key autophagy/lysosomal proteins over time in the exogenous α-synuclein fibril-treated neurons. We observed that temporal changes in the accumulation of cytoplasmic α-synuclein inclusions were associated with changes in the key autophagy/lysosomal markers. Of note, chloroquine-mediated blockade of autophagy increased accumulation of α-synuclein inclusions, and rapamycin-induced activation of autophagy, or use of 5′-AMP–activated protein kinase (AMPK) agonists, promoted the clearance of fibril-mediated α-synuclein pathology. These results suggest a key role for autophagy in clearing fibrillar α-synuclein pathologies in human neuronal cells. We propose that our findings may help inform the development of human neural cell models for screening of potential therapeutic compounds for PD or for providing insight into the mechanisms of α-synuclein propagation. Our results further add to existing evidence that AMPK activation may be a therapeutic option for managing PD.

A hallmark feature of Parkinson's disease (PD)[4] is the neuronal deposition of α-synuclein into proteinaceous inclusions, termed Lewy bodies. After careful assessment of post-mortem PD brains, it is now recognized that α-synuclein Lewy pathology occurs in a characteristic pattern, restricted at first to the brainstem and olfactory bulb and then appearing in limbic and finally neocortical regions over time (1). The progression of α-synuclein pathology is thought to underlie neuronal dysfunction and is associated with the progression of clinical PD symptomology (2). Evidence suggests that the characteristic progression of α-synuclein pathology occurs in a prion-like manner in which misfolded pathological α-synuclein can be taken up by a neuron and trigger the conversion of normal endogenous α-synuclein to the misfolded pathological form (3, 4). Initial evidence for this prion-like propagation of α-synuclein came from assessment of PD patients who had received neurosurgical grafts of fetal dopamine neurons into the basal ganglia, which revealed that α-synuclein had propagated from the patient neurons to the grafted donor neurons (5, 6). Subsequently, pathological fibrillar forms of α-synuclein have been used to demonstrate propagation in cell and animal models of PD (7, 8).

Understandably, there is now much interest from a therapeutic perspective in delineating the mechanisms regulating both the uptake and release of α-synuclein by neurons. The uptake of exogenous α-synuclein fibrils into neurons appears to largely occur via endocytosis (9–12), potentially mediated by cell surface receptors, with LAG3 (13) and cellular prion protein (PrP^C) (14) implicated among candidates to date. Although details remain to be defined, the extracellular release of α-synuclein appears linked to a cell's intrinsic ability to clear the pathological protein via degradation pathways. Macroautophagy, chaperone-mediated autophagy, and the ubiquitin–proteasome system have all been implicated in the clearance of α-synuclein (15–20), and dysfunction of these pathway may promote the extracellular release of α-synuclein (18, 21-23). The extent to which each degradation pathway contributes to α-synuclein clearance and the interplay between these path-

This work was supported by National Health and Medical Research Council (NHMRC) of Australia Grant 1103757. The Dementia and Movement Disorders Laboratory is supported by Forefront, a collaborative research group dedicated to the study of non-Alzheimer disease degenerative disorders, funded by NHMRC Program Grants 1037746 and 1095127. The authors declare that they have no conflicts of interest with the contents of this article.

This article contains Figs. S1–S7.

[1] Supported by a scholarship from the University of New South Wales and later the University of Sydney.

[2] An NHMRC Senior Principal Research Fellow (Grant 1079679).

[3] To whom correspondence should be addressed: Brain and Mind Centre, University of Sydney, Camperdown, New South Wales 2050, Australia. Tel.: 61-2-8627-6054; E-mail: nicolas.dzamko@sydney.edu.au.

[4] The abbreviations used are: PD, Parkinson's disease; AMPK, 5′-AMP–activated protein kinase; IPSC, induced pluripotent stem cell; ACC, acetyl-CoA carboxylase; ULK1, Unc-51–like kinase 1; DPBS, Dulbecco's phosphate-buffered saline; DMEM, Dulbecco's modified Eagle's medium; NSC, neural stem cell; MAP, microtubule-associated protein; LC3, light chain 3; LAMP2, lysosome-associated membrane protein 2; TUJ1, β_3-tubulin; DAPI, 4′,6-diamidino-2-phenylindole; ANOVA, analysis of variance.

ways remains to be fully elucidated; however, it is evident that both the cell type and pathological form of α-synuclein are important (24).

Post-mortem analysis of human brain tissue has uncovered evidence of defective autophagy/lysosomal function in association with α-synuclein pathology (25–27), and major PD risk genes, such as *GBA1* and *LRRK2*, play a role in regulating autophagy/lysosomal pathways (28). These findings add to evidence that targeting the autophagy/lysosomal pathway is a promising therapeutic strategy for the treatment of PD. Indeed, a large body of evidence demonstrates that activation of autophagy pathways reduces α-synuclein levels and affords neuroprotection in various preclinical models (for recent comprehensive reviews, see Refs. 29–32). Despite such evidence, the best therapeutic strategies for activating autophagy as a treatment for PD remain unclear. Again, this is complicated by the effect of different pathological forms of α-synuclein on autophagy pathways and translation of results across different preclinical models. At least one strategy, however, involves activation of autophagy through inhibition of the mammalian target of rapamycin (mTOR) protein. This can be achieved directly with mTOR inhibitors such as rapamycin or indirectly by targeting mTOR-regulating kinases such as protein kinase B (PKB/Akt) or 5′-AMP-activated protein kinase (AMPK) (33).

In the current study, we have investigated α-synuclein inclusions and autophagy/lysosome markers in human neural cells, including primary neurons differentiated from induced pluripotent stem cells. We found evidence for a temporal relationship between neuronal cytoplasmic α-synuclein inclusions and changes in autophagy/lysosome markers following treatment of neurons with exogenous α-synuclein fibrils. This relationship can be modulated in primary human neurons with both inhibitors and activators of the autophagy/lysosome pathway, including small-molecule activators of AMPK, providing a model that can be further interrogated to understand potential mechanisms underlying the propagation of pathological α-synuclein and to evaluate preventive therapeutic strategies.

Results

Temporal changes in α-synuclein inclusion accumulation following treatment of SH-SY5Y cells with PFFs

To assess the relationship between autophagy and α-synuclein, we first prepared exogenous α-synuclein fibrils for treatment. Preformed fibrils (PFFs) were prepared from recombinant monomeric protein, and after 7 days of shaking at 37 °C there was an ~140-fold increase in the fluorescence of thioflavin T (Fig. S1*A*), indicating a strong formation of fibrils. Higher-molecular-weight α-synuclein species could also be clearly seen by immunoblotting (Fig. S1*B*), and EM analysis of the fibrils showed a heterogeneous mixture ranging in size from ~20 to 250 nm (Fig. S1*C*). Having successfully generated exogenous fibrils, we then proceeded to treat differentiated SH-SY5Y neuroblastoma cells with α-synuclein PFFs, or monomeric α-synuclein as a control, and measured α-synuclein inclusion accumulation over a 14-day time course. Inclusions and/or puncta of α-synuclein were clearly visible in PFF-treated cells but not cells treated with the monomeric protein (Fig. 1*A*). We used two concentrations of PFFs, 2 and 5 μg/ml, and for both, the number of α-synuclein inclusions peaked at days 4–6 post-PFF treatment before steadily declining over the rest of the time course (Fig. 1*B*). As well as the number of inclusions, the size of the α-synuclein inclusions also appeared to decline over the time course (Fig. 1*C*). To quantify this, we conducted a particle size analysis, defining small particles as 2–5 μm^2, medium particles as 5–10 μm^2, and large particles as >10 μm^2. This analysis showed that 51% of α-synuclein inclusions were classified as large on day 4, with this declining to 12% by day 14 (Fig. 1*D*). A three-dimensional spatial analysis showed that the α-synuclein inclusions were largely perinuclear (Fig. S2).

Treatment of SH-SY5Y cells with PFFs does not induce cell death within 14 days

We next determined whether changes in α-synuclein inclusion accumulation were related to either cell death or cell proliferation. We treated the differentiated SH-SY5Y cells with the highest concentration of PFFs (5 μg/ml) and stained for the neuronal marker β_3-tubulin (TUJ1). Over 95% of cells strongly expressed TUJ1 over the 14-day time course, demonstrating that the cells were remaining as differentiated neurons (Fig. 2*A*). Crystal violet staining showed that the number of cells was neither increasing nor decreasing throughout the time course, irrespective of PFF treatment (Fig. 2*B*). There was also no difference in the extracellular release of lactate dehydrogenase between untreated and PFF-treated cells over the 14-day time course (Fig. 2*C*). Note that the medium was changed after collection on days 4, 8, and 12 for these experiments, explaining the peaks in Fig. 2*C*. Collectively, these data show that PFF treatment was not inducing cell death within the 14-day time course and that changes in α-synuclein inclusion levels were not due to increasing or decreasing numbers of neuronal cells.

PFF-mediated inclusions contain endogenous α-synuclein

We also aimed to confirm that the inclusions observed following PFF treatment contained endogenous α-synuclein. To achieve this, we used CRISPR-Cas9–mediated genome editing to generate α-synuclein–knockout SH-SY5Y cells. Following clonal selection, immunoblotting for α-synuclein demonstrated the successful generation of these cells (Fig. 2*D*). Importantly, the knockout cells showed vastly reduced α-synuclein inclusion immunostaining at 6 days post-PFF treatment (Fig. 2*E*). We were also able to detect low levels of Ser-129–phosphorylated α-synuclein in PFF-treated SH-SY5Y cells but not in α-synuclein–knockout cells (Fig. 2*F*). Collectively these results indicate that endogenous α-synuclein is incorporated into the exogenous fibril-mediated inclusions.

Temporal changes in autophagy markers follow treatment of SH-SY5Y cells with PFFs

Based on the initial temporal α-synuclein inclusion results, we next chose to analyze autophagy markers at 4, 6, and 8 days post-treatment of differentiated SH-SY5Y cells with 2 μg/ml PFFs. Again, there was a peak in α-synuclein inclusions at day 6 post-PFF treatment, with a significant reduction from the peak observed by day 8 (Fig. 3*A*). These temporal changes in cytoplasmic α-synuclein inclusions were associated with increases

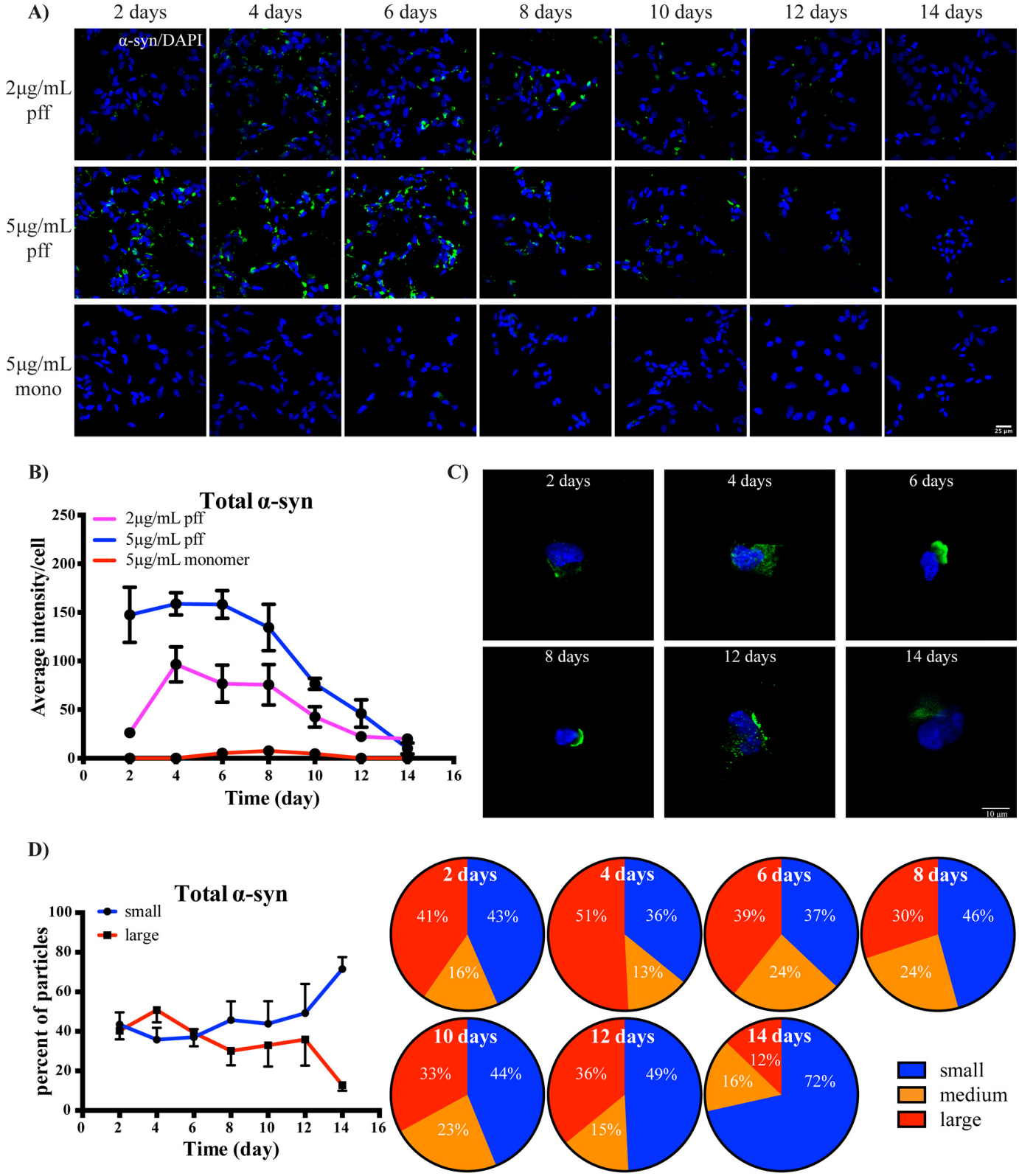

Figure 1. Temporal changes in cytoplasmic α-synuclein inclusions following treatment of SH-SY5Y cells with PFFs. *A*, SH-SY5Y cells were treated with PFFs or α-synuclein monomer as indicated and then fixed for immunofluorescence staining of total α-synuclein (*green*) at the indicated time points. The *blue* is DAPI staining. Images were taken at 40× objective *magnification*. The *scale bar* is 25 μm. *B*, average intensity of particles >2 μm² per cell were compared between PFF- and monomer-treated groups over time. Up to eight images, each containing 50–100 cells per image, were analyzed for each treatment condition. Data are shown as mean ± S.D. (*error bars*). *C*, representative images taken at 100× *magnification* show the morphology of α-synuclein inclusions (*green*) in SH-SY5Y cells treated with 5 μg/ml PFFs. The *scale bar* is 10 μm. *D*, the relative percentage of small (2–5 μm²), medium (5–10 μm²), and large (>10 μm²) α-synuclein (*α-syn*) inclusions in SH-SY5Y cells treated with 5 μg/ml PFFs and fixed at each time point are shown in the pie charts, with the quantified comparison between treatment groups shown in line graph as mean ± S.D. (*error bars*). Four to eight images were analyzed for each time point.

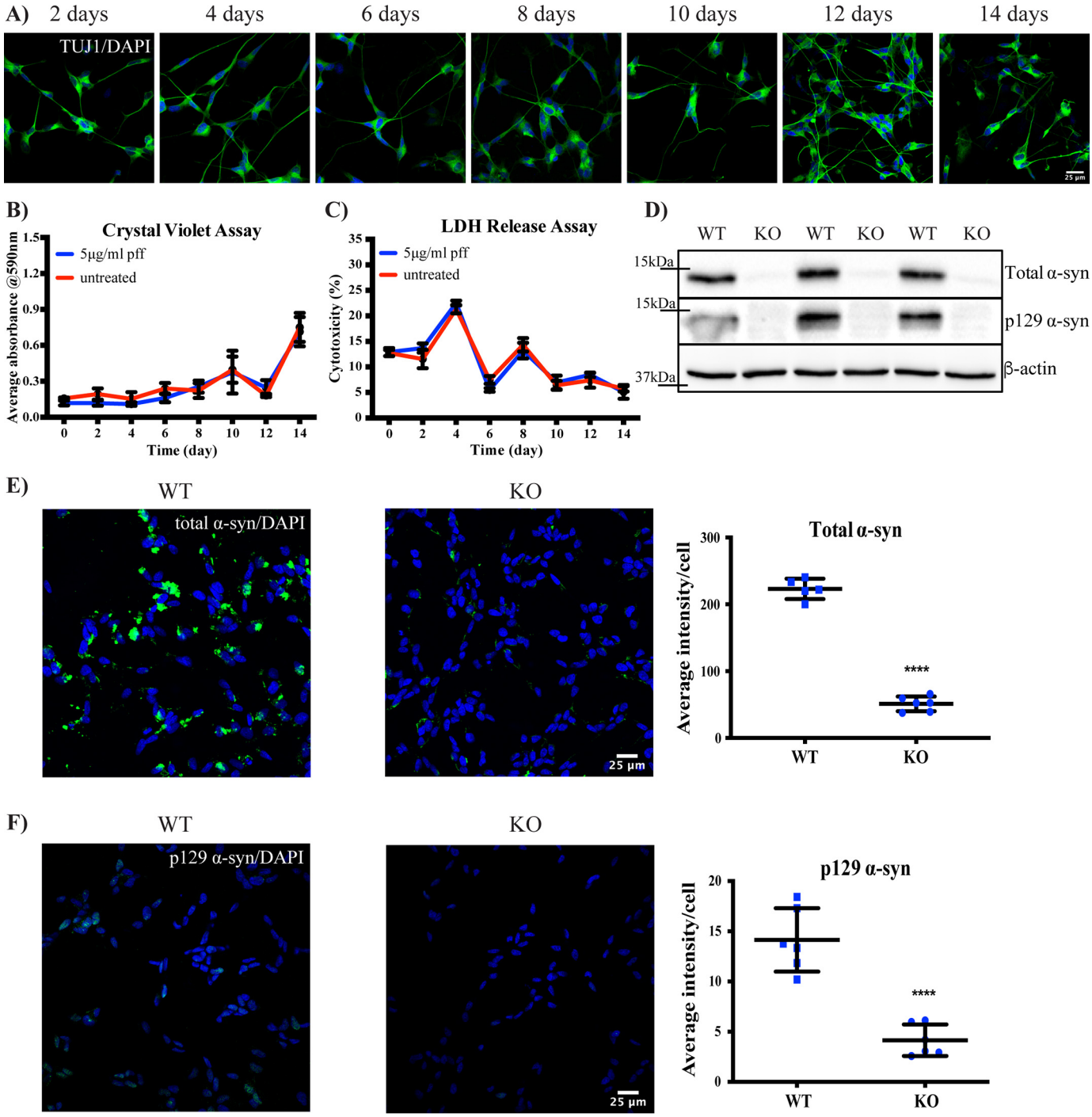

Figure 2. Cell toxicity and antibody specificity in SH-SY5Y cells treated with PFFs. *A*, differentiated SH-SY5Y cells were treated with 5 μg/ml PFFs, fixed at the indicated time points, and immunostained for β_3-tubulin staining (*green*). The *blue* stain is DAPI. Images were taken at 40× objective *magnification*. The *scale bar* is 25 μm. *B*, the viability of SH-SY5Y cells after treatment with 5 μg/ml PFFs over time was measured by crystal violet assay. Results are shown as mean absorbance ±S.D. (*error bars*). *C*, lactate dehydrogenase levels in SH-SY5Y cells after treatment with 5 μg/ml PFFs over time was measured using a colorimetric cytotoxicity assay. Results are shown as the mean percentage of cytotoxicity to maximum lactate dehydrogenase release ±S.D. (*error bars*). *D*, WT and α-synuclein–knockout (*KO*) SH-SY5Y cells lysates were used to immunoblot for total and Ser-129–phosphorylated α-synuclein (*α-syn*), with β-actin as a loading control. WT and α-synuclein–knockout SH-SY5Y cells were treated with 5 μg/ml PFFs and after 6 days immunostained for total α-synuclein (*green*) (*E*) or Ser-129–phosphorylated α-synuclein (*F*). The *blue* stain is DAPI. The graph shows the mean intensity of total or phosphorylated α-synuclein per cell ±S.D. (*error bars*). Student's *t* test was used to compare knockout cells with WT. For all images, the *scale bar* is 25 μm. All experiments were performed at least twice with all assays at least in triplicate.

in the autophagy markers p62 and light chain 3 (LC3) and the lysosomal protein lysosome-associated membrane protein 2 (LAMP2), which all peaked at day 6 and then significantly declined by day 8 (Fig. 3, *B–D*). None of these autophagy/lysosomal proteins changed over the same time course in untreated SH-SY5Y cells (Fig. 3, *B–D*). These results suggest that PFF treatment causes a transient block in either the formation or degradation of autolysosomes.

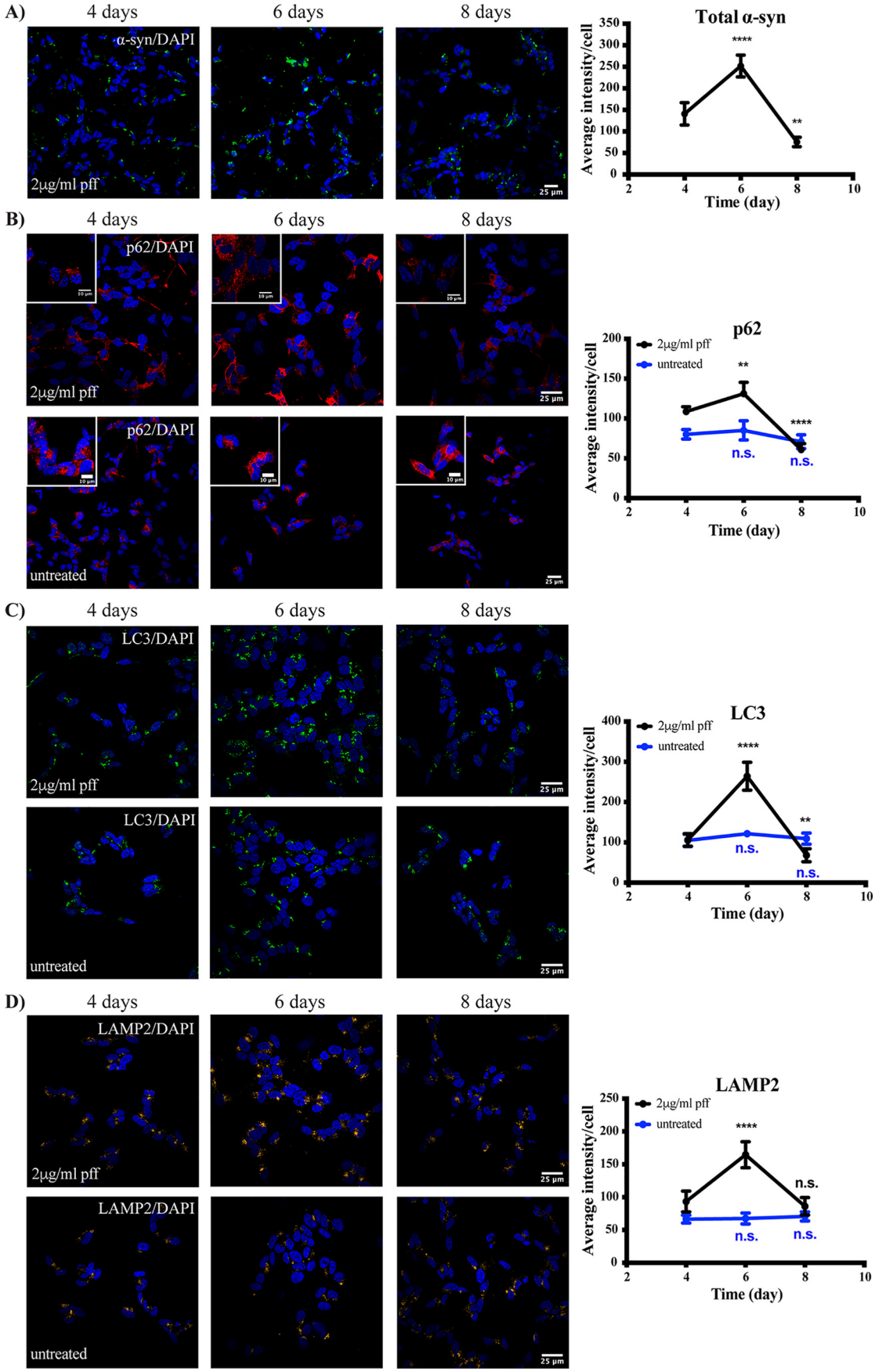
A)
4 days
6 days
8 days
α-syn/DAPI
2μg/ml pff
Total α-syn
Average intensity/cell
Time (day)
B)
p62/DAPI
2μg/ml pff
untreated
p62
2μg/ml pff
untreated
n.s.
C)
LC3/DAPI
LC3
D)
LAMP2/DAPI
LAMP2
25 μm

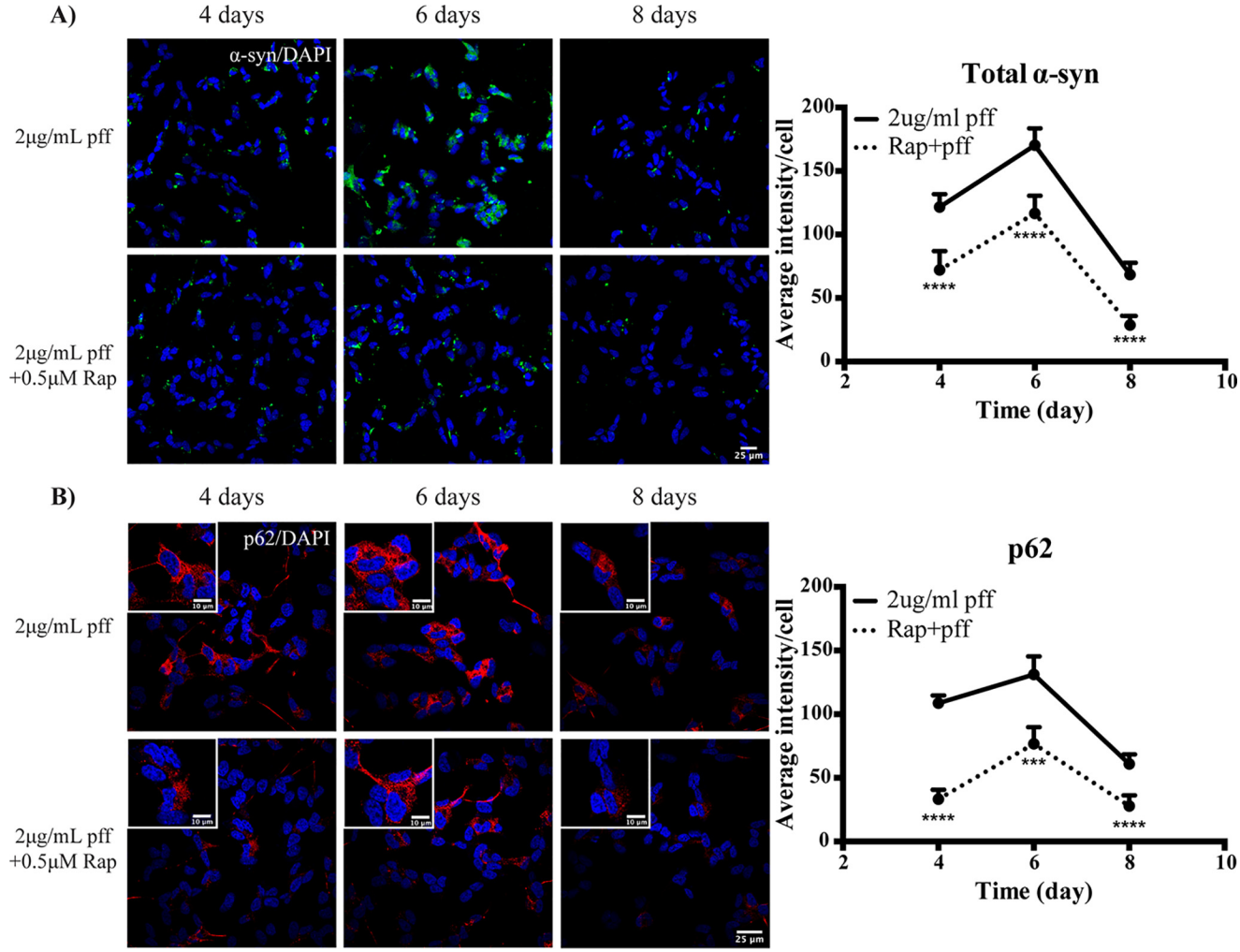

Figure 4. Activation of autophagy promotes α-synuclein inclusion clearance in SH-SY5Y cells. Differentiated SH-SY5Y cells were treated with 2 μg/ml PFFs in the presence or absence of 0.5 μM rapamycin (*Rap*) for up to 8 days. Images were taken at 40× *magnification* for the analysis of total α-synuclein (*α-syn*) immunofluorescence (*green*) (*A*) and at 60× *magnification* for the analysis of p62 immunofluorescence (*red*) (*B*). *Scale bars* are 25 μm (10 μm in *insets*). The *blue* stain is DAPI. Four to eight images containing 50–100 cells per image were analyzed for each time point. Graphs show the mean intensity per cell ±S.D. (*error bars*). Student's *t* test was used to compare ±rapamycin-treated groups at each time point. ***, $p < 0.001$; ****, $p < 0.0001$.

Activation of autophagy reduces α-synuclein inclusion accumulation following treatment of SH-SY5Y cells with PFFs

We next aimed to determine whether activation of autophagy could reduce the accumulation of α-synuclein inclusions following PFF treatment. To achieve this, we treated cells with 2 μg/ml PFFs in the presence or absence of 0.5 μM rapamycin for up to 8 days. At all time points studied, rapamycin treatment significantly reduced the accumulation of α-synuclein inclusions induced by PFF treatment (Fig. 4*A*). This was associated with a significant reduction in the levels of p62 with rapamycin treatment at all time points studied (Fig. 4*B*). As rapamycin may affect protein synthesis, we also performed a more acute 48-h rapamycin treatment, adding the rapamycin to cells that had already been exposed to PFFs for 6 days. Analysis of the resulting 8-day time point showed that rapamycin could still significantly reduce the accumulation of α-synuclein inclusions (Fig. S3).

Blockade of autophagy increases α-synuclein inclusion accumulation in SH-SY5Y cells

To determine whether blocking the degradation of autophagolysosomes could prevent the reduction in α-synuclein inclusions, we next treated differentiated SH-SY5Y cells with 2 μg/ml PFFs, and after 6 days the cells were treated for an additional 48 h with or without 20 μM chloroquine. At the resulting 8-day time point, the number of α-synuclein inclusions remained significantly higher in the chloroquine-treated cells compared with those not treated with chloroquine (Fig. 5*A*). The increased number of α-synuclein

Figure 3. Temporal changes in autophagy markers following treatment of SH-SY5Y cells with PFFs. Differentiated SH-SY5Y cells were treated with or without 2 μg/ml α-synuclein PFFs and fixed for immunofluorescence at the time points indicated. Cells were immunostained for total α-synuclein (*α-syn*) (*green*) (*A*), SQSTM1/p62 (*red*) (*B*), LC3 (*green*) (*C*), or LAMP2 (*yellow*) (*D*). *Scale bars* are 25 μm (10 μm in *insets*). The *blue* stain is DAPI. Four to eight images containing 50–100 cells per image were analyzed for each time point. Graphs show the mean intensity of each marker per cell ±S.D. (*error bars*). One-way ANOVA was used to compare later time points with day 4. **, $p < 0.01$; ****, $p < 0.0001$; *n.s.*, not significant.

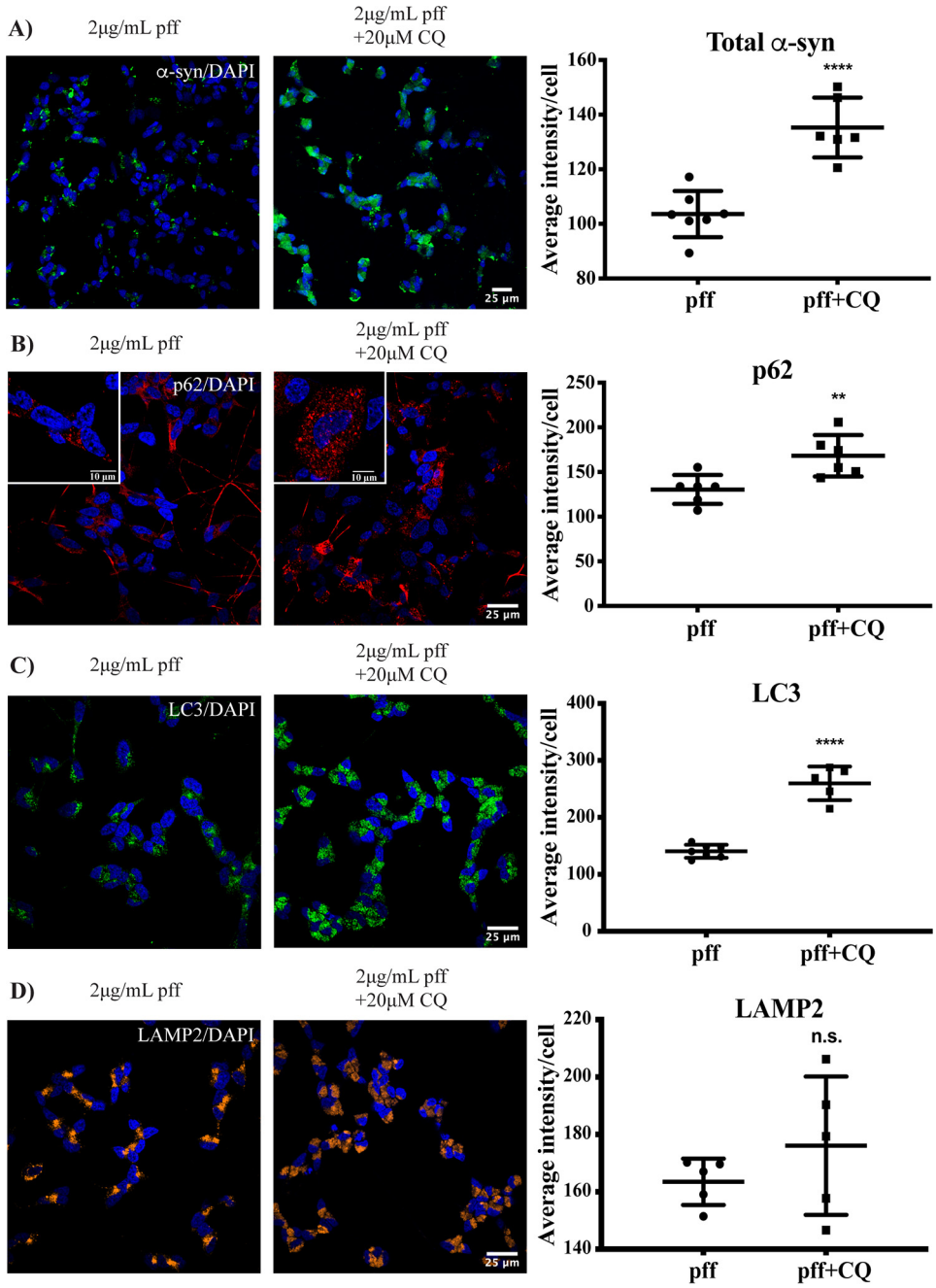

Figure 5. Blockade of autophagy prevents α-synuclein inclusion clearance in SH-SY5Y cells. Differentiated SH-SY5Y cells were treated with 2 μg/ml α-synuclein (*α-syn*) PFFs, and after 6 days cells were incubated in the presence or absence of 20 μM chloroquine (*CQ*) for a further 48 h. Images were taken at 40× *magnification* for the analysis of total α-synuclein immunofluorescence (*green*) (*A*) and at 60× *magnification* for the analysis of p62 immunofluorescence (*red*) (*B*), LC3 immunofluorescence (*green*) (*C*), or LAMP2 immunofluorescence (*yellow*) (*D*). *Scale bars* are 25 μm (10 μm in *insets*). The *blue* stain is DAPI. Four to eight images containing 50–100 cells per image were analyzed for each condition. Graphs show the mean intensity per cell ±S.D. (*error bars*). Student's *t* test was used to compare the ±chloroquine groups. **, $p < 0.01$; ****, $p < 0.0001$; *n.s.*, not significant.

inclusions was again associated with an increase in both p62 (Fig. 5*B*) and LC3 (Fig. 5*C*) in the chloroquine-treated cells, whereas LAMP2 remained similar under these conditions (Fig. 5*D*). We were unable to culture the neuronal cells for longer than 48 h with any effective dose of chloroquine due to toxicity. Collectively, these results suggest that autophagy is important for clearing α-synuclein inclusions following the treatment of differentiated SH-SY5Y cells with exogenous α-synuclein fibrils.

Temporal changes in α-synuclein inclusions and p62 accumulation following treatment of induced pluripotent stem cell (IPSC)-derived neurons with PFFs

To determine whether a similar reliance on autophagy for the clearance of fibril-mediated α-synuclein inclusions also occurred in primary human neurons, we used IPSC-derived human neural stem cells and differentiated them to neurons as we have reported previously (34). After 7 days of differentiation, the primary neurons were treated with 2 or 5 μg/ml of PFFs, as

well as 5 μg/ml monomeric α-synuclein as a control, and cultured for up to 12 days. The α-synuclein was only added once, and a half medium change was performed every 48 h. Greater than 90% of cells stained positive for the neuronal markers microtubule-associated protein 2 (MAP2) and TUJ1, and this did not change over the PFF treatment time course (Fig. S4*A*). Treatment of the IPSC-derived neurons with PFFs, but not monomeric α-synuclein, resulted in an increase in cytoplasmic α-synuclein inclusions (Fig. 6*A*) and increased levels of p62 (Fig. 6*B*). Quantification again demonstrated that the cytoplasmic accumulation of α-synuclein inclusions (Fig. 6*C*) and p62 (Fig. 6*D*) peaked at day 6, before declining over the rest of the time course. Again, the α-synuclein inclusions were predominantly perinuclear (Fig. S4B). Treating the IPSC-derived neurons with 5 μg/ml PFFs did not affect cell viability over the time course when measured by either crystal violet staining (Fig. S4*C*) or lactate dehydrogenase release (Fig. S4*D*). As for SH-SY5Y cells, Ser-129–phosphorylated α-synuclein inclusions could also be detected in the IPSC-derived neurons following PFF treatment (Fig. S4*E*).

Small-molecule AMPK activators promote α-synuclein inclusion clearance in SH-SY5Y cells

Activation of AMPK can promote autophagy, and AMPK has been suggested as a potential therapeutic target for PD (35). We therefore assessed whether small-molecule AMPK activators could promote the clearance of the cytoplasmic α-synuclein inclusions observed following PFF treatment. Dose-response experiments using SH-SY5Y cells demonstrated that 5 and 30 μM GSK621 and A769662, respectively, could activate AMPK using phosphorylation of the AMPK substrate acetyl-CoA carboxylase (ACC) at Ser-79 as a readout (Fig. 7, *A* and *B*). At these concentrations, both compounds could also induce the phosphorylation of the downstream AMPK substrate and autophagy-activating kinase Unc-51–like kinase 1 (ULK1), indicating that AMPK activation can initiate this autophagy-regulating pathway in the SH-SY5Y cells (Fig. 7, *C* and *D*). Importantly, both compounds could reduce levels of α-synuclein inclusions at 6 days post-PFF treatment (Fig. 7*E*), and this was again associated with a significant reduction in p62 (Fig. 7*F*). Again, we also performed a more acute treatment, adding the AMPK agonists to cells for 48 h after they had been treated with PFFs for 6 days. Both AMPK agonists still significantly reduced α-synuclein inclusions under these conditions (Fig. S5). Moreover, the ability of AMPK agonists to reduce PFF-mediated α-synuclein inclusions was prevented with the addition of chloroquine (Fig. S6), implicating autophagy/lysosomal clearance as the main mechanism of action for these compounds. Finally, with the concentrations employed, we could find no evidence that AMPK agonists could induce phosphorylation of α-synuclein at Ser-129, and AMPK agonist treatment alone did not induce α-synuclein inclusions in SH-SY5Y cells (Fig. S7).

Small-molecule 5′-AMP–activated protein kinase (AMPK) activators promote α-synuclein inclusion clearance in IPSC-derived neurons

Finally, we assessed whether the AMPK activators could promote the clearance of α-synuclein inclusions in the IPSC-derived neurons. Again, both compounds significantly reduced α-synuclein inclusion levels at 6 days post-PFF treatment (Fig. 8*A*). In addition to reduced levels of α-synuclein inclusions, treatment of the IPSC-derived neurons with AMPK activators also resulted in a significant decrease in the levels of p62 (Fig. 8*B*), LC3 (Fig. 8*C*), and LAMP2 (Fig. 8*D*) compared with the PFF alone–treated cells.

Discussion

In the current study, we investigated the temporal relationship between the cytoplasmic accumulation of α-synuclein inclusions and the lysosomal/autophagy pathway in human neural cell lines following treatment with exogenous α-synuclein fibrils. We consistently found a robust accumulation of α-synuclein inclusions at 4–6 days post-treatment, and this was associated with an increase in the autophagy marker p62. After this time, p62 returned toward baseline, and the number of α-synuclein inclusions declined. Lysosomal inhibition with chloroquine prevented the clearance of cytoplasmic α-synuclein inclusions, whereas activation of autophagy with both rapamycin and activators of AMPK promoted the clearance of α-synuclein inclusions. These results provide evidence of a dynamic relationship between autophagy and the cytoplasmic accumulation of α-synuclein in human neurons, with potential implications for understanding the propagation of α-synuclein pathology in PD.

One finding was that fibril-induced α-synuclein inclusions were largely cleared from the human neural cells and did not induce toxicity over the time course studied. This result is consistent with a study that used mixed neuronal/glial cultures from mice and showed that internalized fibrils could seed endogenous α-synuclein inclusions, and these were effectively cleared by autophagy pathways (36). However, a sustained induction of α-synuclein pathology following exogenous fibril treatment leading to neurotoxicity within 14 days has also been reported for primary mouse neurons (11). Thus, despite a growing consensus regarding the importance of autophagy for clearing pathological α-synuclein, the ability to clear α-synuclein inclusions and prevent toxicity may differ across models. A number of factors are thought to contribute to α-synuclein toxicity following fibril treatment. These include the levels of endogenous α-synuclein (37), with overexpression of α-synuclein promoting fibril-mediated toxicity (38–40), and the preparation of the exogenous α-synuclein fibrils, with shorter, <50-nm fibrils promoting toxicity (41, 42). The aim of our current study was to assess fibril-mediated α-synuclein pathology under endogenous levels of α-synuclein expression in human neurons, including primary neurons derived from a healthy individual. Under these conditions, our results suggest that human neurons are capable of clearing α-synuclein inclusions and are not susceptible to fibril-mediated toxicity. It would be of interest however, to use this model to determine whether α-synuclein inclusions clearance is perturbed in neurons derived from PD patients, including in neurons derived from patients with mutations in PD risk genes known to alter lysosomal/autophagy function such as *GBA1* and *LRRK2*.

In support of the important role for autophagy in the clearance of α-synuclein inclusions are imaging studies showing that that the majority of internalized α-synuclein fibrils are traf-

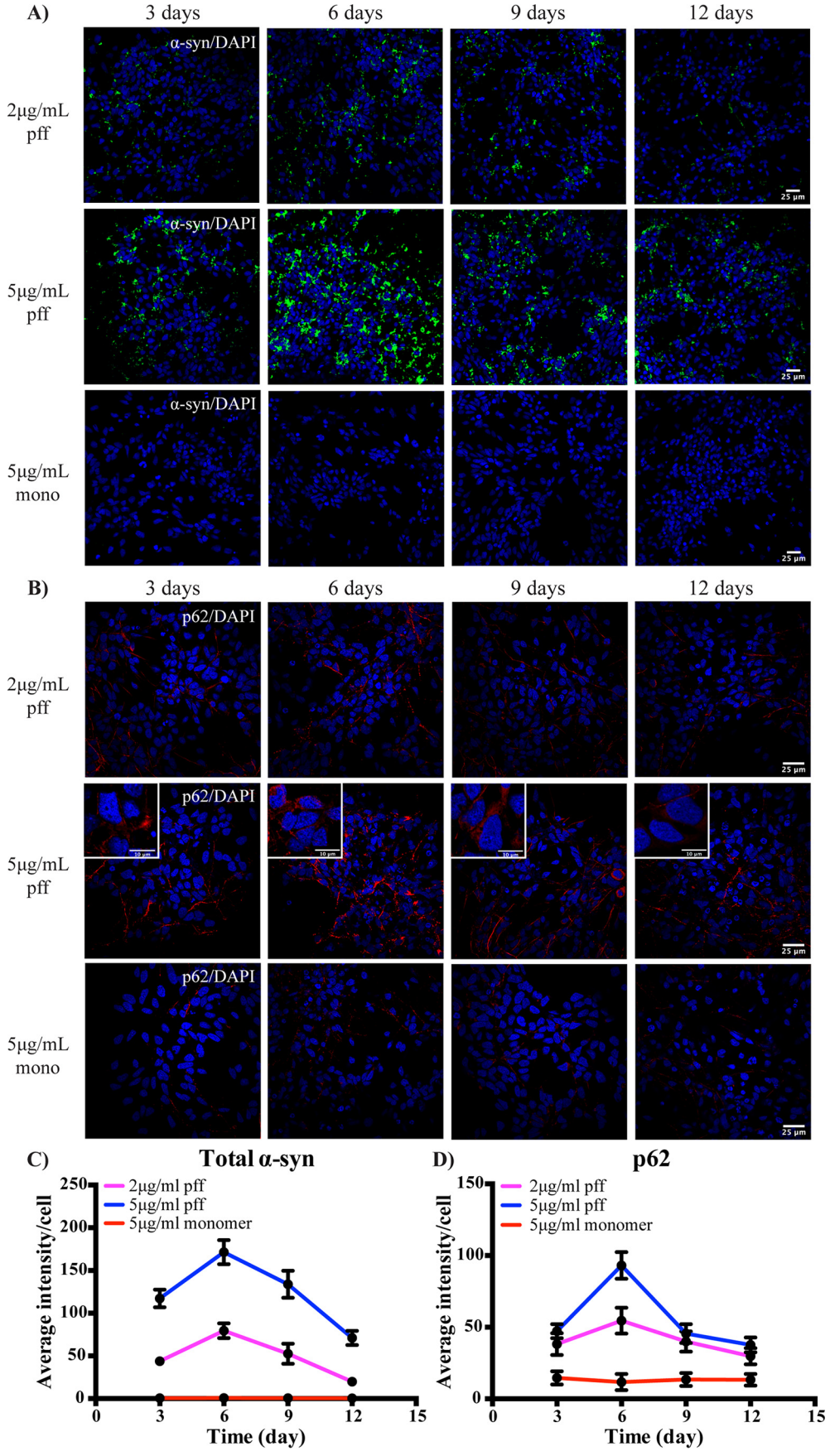
A)
3 days
6 days
9 days
12 days
α-syn/DAPI
2μg/mL pff
5μg/mL pff
5μg/mL mono
B)
p62/DAPI
C)
Total α-syn
Average intensity/cell
2μg/ml pff
5μg/ml pff
5μg/ml monomer
Time (day)
D)
p62

ficked to the lysosome for clearance (36, 43). In regard to the prion-like spreading hypothesis of α-synuclein, this still leaves important questions such as how exactly do pathogenic fibrils seed conversion of endogenous α-synuclein inclusions and how does this lead to impairments in the autophagy/lysosome pathway. Evidence suggests that α-synuclein fibrils are resistant to lysosomal degradation, and they have been shown to persist in the lysosomes of primary mouse neurons for up to 7 days (43). α-Synuclein fibrils are also efficient at rupturing and escaping from lysosomes, facilitating interaction with endogenous α-synuclein (44). The inefficient clearance of α-synuclein can also lead to the accumulation of truncated neurotoxic species in mice (45). In the current study, although the majority of the α-synuclein inclusions were cleared within 7 days, we still observed some inclusions after 2 weeks. Whether these represent a degradation-resistant α-synuclein conformation capable of inducing Lewy pathology over a longer time course remains to be determined. Further work is also required to determine mechanisms behind the changes in autophagy following fibril treatment. Our results may simply suggest a transient overwhelming of the autophagy/lysosomal system by the internalized fibrils. However, that we could further activate autophagy to increase α-synuclein inclusion clearance suggests a mechanism more complex than just overwhelming the intrinsic capacity of the autophagy/lysosome system. In this regard, α-synuclein has been directly implicated in the inhibition of autophagy and in particular the inhibition of protein-trafficking pathways important for autophagy (46–49). Employing more dynamic measures of autophagy/lysosomal function in our human cell models may provide further mechanistic insight in this regard.

Finally, we also demonstrated that two different small-molecule activators of AMPK could promote the clearance of α-synuclein inclusions following fibril treatment, and this was associated with improvements in autophagy. AMPK activation stimulates macroautophagy via direct phosphorylation of ULK1, leading to the induction of autophagosome formation (50). Previous studies in cells and rodents have shown that AMPK activation can promote the autophagic clearance of overexpressed α-synuclein and reduce neurotoxicity (51–53), although chronic hyperactivation of AMPK may actually contribute to α-synuclein pathology (54, 55). Our results using fibril-treated primary human neurons suggest that small-molecule activation of AMPK at the concentrations employed is beneficial in regard to α-synuclein pathology. It would thus be of merit to further demonstrate using genetic or other means that increased autophagy is the mechanism by which AMPK activation promotes α-synuclein inclusion clearance in our model. It would also be of interest to determine whether AMPK activation remains efficacious in neural cell lines from PD patients where autophagy/lysosomal function may be perturbed.

Experimental procedures

Preparation of α-synuclein PFFs

Human recombinant α-synuclein monomeric protein at 13.2 mg/ml in 10 mM Tris and 50 mM NaCl, pH 7.6, was purchased from Proteos, and PFFs were prepared as outlined (42). Briefly, α-synuclein monomer was centrifuged at 12,000 × *g* in a benchtop centrifuge for 10 min. The supernatant was collected, and the protein concentration was determined by NanoDrop. Monomeric protein was then diluted to 5 mg/ml in sterile Dulbecco's phosphate-buffered saline (DPBS) (Ca^{2+}-, Mg^{2+}-free; Gibco) and continuously shaken at 1,000 rpm on an orbital shaker (Thermomix) placed in a 37 °C incubator for 7 days. After this time, the presence of amyloid fibrils was confirmed by thioflavin T assay. For this assay, thioflavin T (Sigma) was diluted to 25 μm in DPBS; then mixed with 2.5 μl of fibrillar α-synuclein, or monomeric α-synuclein as a control, in a black 96-well microplate (Greiner); and incubated at room temperature for 5 min. After incubation, the plate was read with excitation and emission settings of 450 and 480 nm, respectively, using a CLARIOstar plate reader (BMG Labtech). 25 μl aliquots of fibrillar α-synuclein were then stored at −80 °C. PFFs were stored for up to 1 year before being replaced. Three identically prepared batches of PFFs were used to complete the study. Immediately before treating the cells, the aggregated α-synuclein was diluted in sterile DPBS to 0.1 mg/ml and sonicated for 30 s at 40% amplitude and 1-s on/off pulse durations (Q125, Q Sonica) to generate PFFs. The PFFs were then further diluted to a working concentration with prewarmed tissue culture medium and immediately applied to cells.

EM analysis of PFFs

For transmission EM, 3 μl of 0.1 mg/ml sonicated or unsonicated PFF samples were applied to glow-discharged 200-mesh, carbon-only, copper grids (Electron Microscopy Sciences) and negatively stained with 2% uranyl acetate (Polysciences), and images captured as we have described previously (56).

SH-SY5Y cell culture and treatment

Human neuroblastoma SH-SY5Y cells were maintained in Dulbecco's modified Eagle's medium/Ham's F-12 supplemented with 10% low endotoxin fetal bovine serum, 2 mM L-glutamine, and 1% penicillin-streptomycin (all from Gibco, Thermo Fisher). For experiments, cells were plated onto coverslips coated with Geltrex matrix (Thermo Fisher) in 12-well plates at a density of 5×10^4 cells/well and incubated overnight. Cells were then differentiated in DMEM/Ham's F-12 supplemented with 1% fetal bovine serum, 1% penicillin-streptomycin, and 10 μM retinoic acid (Sigma) for 4 days before a once-off treatment with PFFs or monomeric α-synuclein at the indicated concentrations. Cells were then

Figure 6. Transient changes in α-synuclein inclusions and autophagy in IPSC-derived neurons treated with PFFs. Differentiated IPSC-derived neurons were treated with 2 or 5 μg/ml PFFs or α-synuclein (*α-syn*) monomer. Cells were fixed at the indicated time points for immunofluorescence analysis of total α-synuclein (*green*; 40× *magnification*) (*A*) and p62 (*red*; 60× *magnification*) (*B*). *Scale bars* are 25 μm (10 μm in *insets*). The *blue* stain is DAPI. Four to eight images containing 50–100 cells per image were analyzed for each condition. The average intensity of α-synuclein (*C*) or p62 (*D*) immunofluorescence was determined for the PFF- and monomer-treated groups. Results are shown in the graphs as mean ± S.D. (*error bars*).

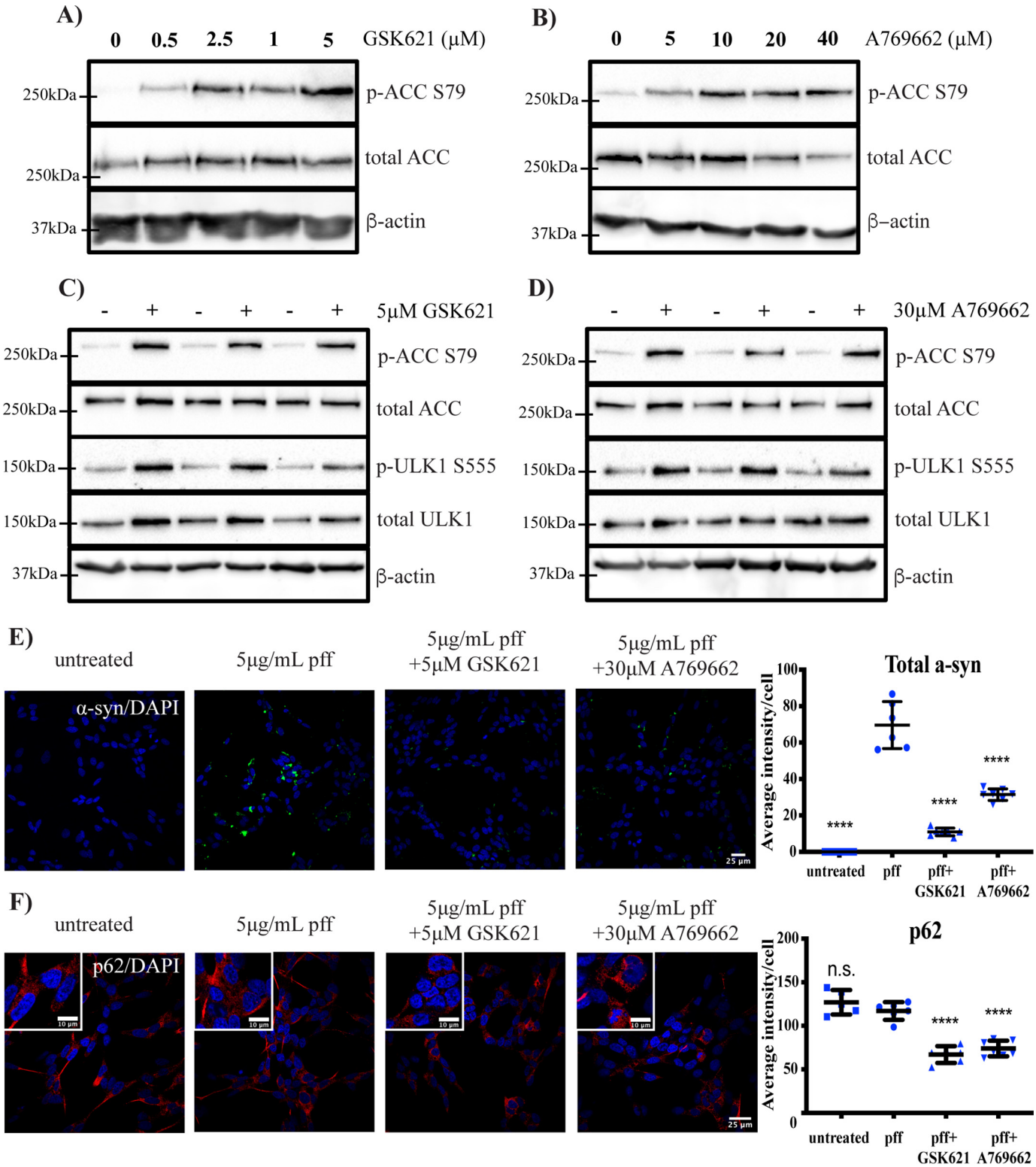

Figure 7. AMPK agonists promote α-synuclein inclusion clearance in SH-SY5Y cells. Differentiated SH-SY5Y cells were treated with the indicated concentrations of AMPK agonist GSK621 (*A*) or A769662 (*B*) for 5 h before immunoblotting for the indicated proteins. Representative immunoblots are shown from at least three independent experiments. Differentiated SH-SY5Y cells were treated with or without 5 μM GSK621 (*C*) or 30 μM A769662 (*D*) for 5 h before immunoblotting for the indicated proteins. Representative immunoblots are shown from at least three independent experiments. Differentiated SH-SY5Y cells were treated with 5 μg/ml PFFs in the presence or absence of 5 μM GSK621 or 30 μM A769662 for 6 days. Cells were fixed and immunostained for total α-synuclein (*α-syn*) (*green*) (*E*) or p62 (*red*) (*F*). *Scale bars* are 25 μm (10 μm in *insets*). The *blue* stain is DAPI. Confocal images are representative of seven images containing 50–100 cells per image that were used for analysis of staining intensity, with quantified results in the graphs showing mean intensity per cell ±S.D. (*error bars*). One-way ANOVA with Tukey's post hoc test was used for comparison. ****, $p < 0.0001$; *n.s.*, not significant.

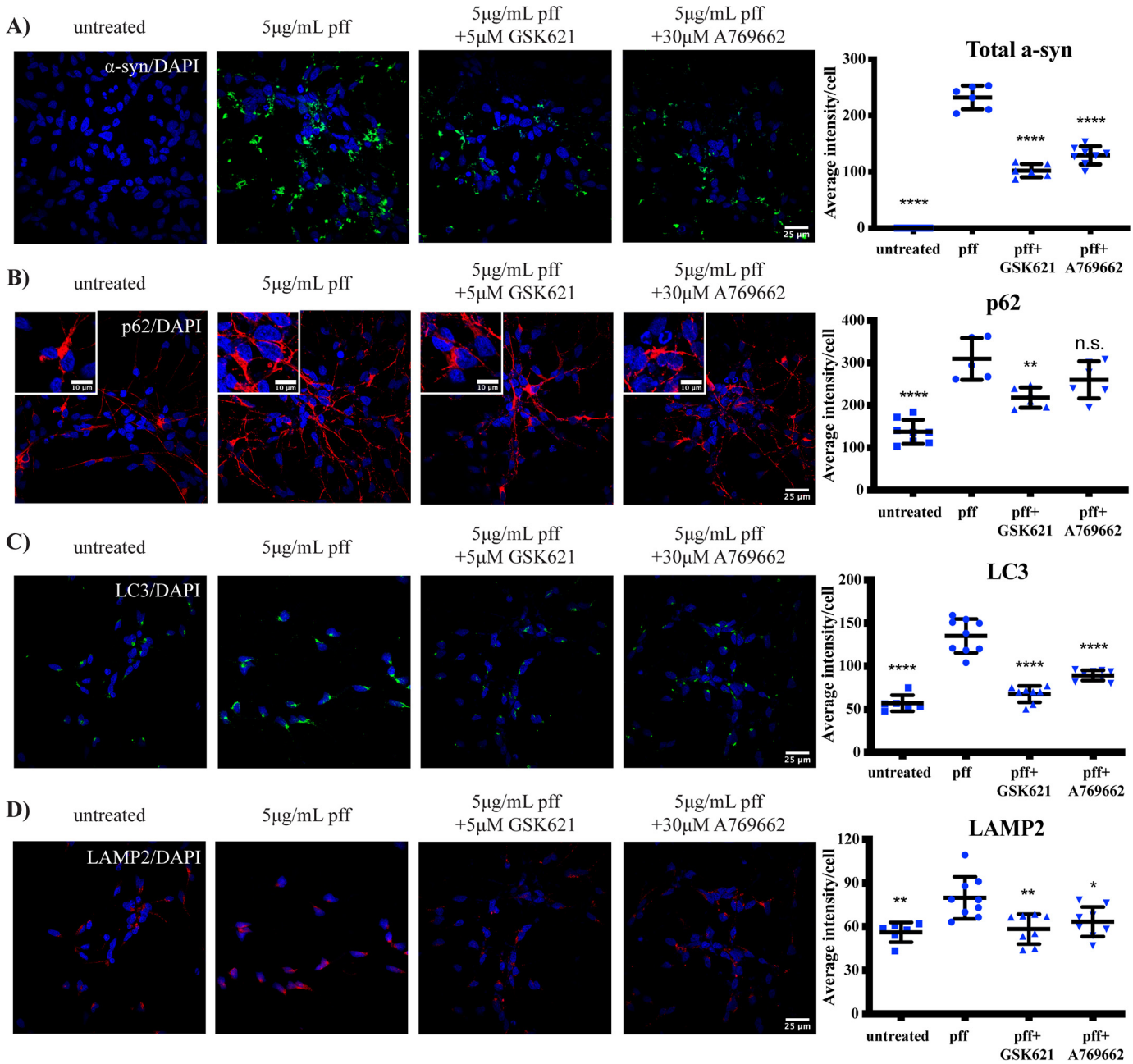

Figure 8. AMPK agonists promote α-synuclein inclusion clearance in IPSC-derived neurons. Differentiated IPSC-neurons were treated with 5 μg/ml PFFs and with or without 5 μM GSK621 or 30 μM A769662. After 6 days, cells were fixed and immunostained for total α-synuclein (*α-syn*) (*green*) (*A*), p62 (*red*) (*B*), LC3 (*green*) (*C*), or LAMP2 (*red*) (*D*). *Scale bars* are 25 μm (10 μm in *insets*). The *blue* stain is DAPI. Confocal images are representative of seven images containing 50–100 cells per image that were used for analysis of staining intensity, with quantified results in the graphs showing mean intensity per cell ±S.D. (*error bars*). One-way ANOVA with Tukey's post hoc test was used for comparison. *, $p < 0.05$; **, $p < 0.01$; ****, $p < 0.0001$; *n.s.*, not significant.

maintained for up to 12 days further, with media replaced every 4 days. Rapamycin and chloroquine were purchased from Sigma and used at the concentrations indicated in the figures. AMPK activators (GSK621 and A769662) were purchased from Cayman Chemicals and used at the concentrations indicated in the figures.

Generation of α-synuclein–knockout SH-SY5Y cells

To make α-synuclein–knockout cells, 100 ng of predesigned GFP-tagged CRISPR-Cas9 plasmids with guide RNA sequences targeting human α-synuclein (Horizon) were amplified in DH5α *E. coli* and purified using PureLink plasmid DNA purification kits (Thermo Fisher). Restriction enzyme digests using EcoRV (New England Biolabs) were performed on purified plasmid DNA to confirm correct isolation. A genomic cleavage detection kit (GeneArt, Thermo Fisher) was used according to the manufacturer's instructions to identify the plasmid most efficient at targeting and cleaving the gene of interest. 2 μg of the identified optimal CRISPR-Cas9 plasmid were then transfected into SH-SY5Y cells using Lipofectamine 3000 (Thermo Fisher). FACS (BD Influx) was used to plate successfully transfected GFP-positive cells into 96-well plates for clonal expan-

sion. Expanded clones were screened for knockout by immunoblotting for α-synuclein.

Induced-pluripotent stem cell–derived neural cell culture and treatment

Experiments employing human induced pluripotent stem cells were approved by the University of Sydney Human Research Ethics Committee (number 2017/094). IPSCs were reprogrammed from primary human fibroblasts of a neurologically normal subject using the Epi5 reprogramming kit (Life Technologies), and then neural stem cells (NSCs) were subsequently derived from the IPSCs using the PSC neural induction kit (Life Technologies). The initial characterization of these cells has been described previously (34). NSCs were cultured in neural expansion medium composed of 50% advanced DMEM and 50% neurobasal medium supplemented with neural induction supplement at 1:50 dilution and 1× penicillin-streptomycin (all from Gibco, Thermo Fisher). The medium was changed every 2 days, and NSCs were passaged in the presence of 10 μl/ml RevitaCell supplement (Thermo Fisher). For experiments, NSCs were plated on coverslips coated with poly-L-ornithine (20 μg/ml; Sigma) and laminin (10 μg/ml; Thermo Fisher) in 12-well plates at a density of 2.5×10^4 cells/well. NSCs were then differentiated to neurons using neurobasal medium supplemented with 2% B-27 serum-free supplement, 2 mM L-glutamine, and 1% penicillin-streptomycin (all from Gibco, Thermo Fisher) as we have described previously (34). Half of the differentiation medium was replaced every 2nd day. The indicated concentration of PFFs or monomeric α-synuclein was added once on day 7 of differentiation, and neurons were maintained for up to 12 days further.

Fluorescence microscopy

Cells on coverslips were washed in 1× PBS and fixed in 4% paraformaldehyde at room temperature for 20 min. After fixing, coverslips were washed with 1× PBS again and then permeabilized with 0.5% saponin (Sigma) for 15 min. Cells were then blocked in 3% bovine serum albumin (BSA) at room temperature for 1 h followed by incubation in primary antibodies at 4 °C overnight. Primary antibodies used were mouse monoclonal α-synuclein (BD Biosciences, 610787; 1:200), mouse monoclonal phospho-α-synuclein (Ser-129, 81A) (BioLegend, 825701; 1:100), rabbit polyclonal MAP2 (Abcam, 32454; 1:300), rabbit polyclonal TUJ1 (Abcam, 18207; 1:300), rabbit monoclonal microtubule-associated proteins 1A/1B LC3A (Abcam, 52768; 1:200), rabbit monoclonal SQSTM1/p62 (Cell Signaling Technology, 7695s; 1:400), and mouse monoclonal LAMP2 (Abcam, 25631; 1:200). Secondary antibodies were donkey anti-mouse Alexa Fluor 488/594 and donkey anti-rabbit Alexa Fluor 488/594 (Life Technologies; 1:400). All of the antibodies were diluted in 3% BSA and 0.5% saponin. Following primary antibody incubation, cells were washed 3 × 5 min in 1× PBS and incubated with Alexa Fluor secondary antibodies at room temperature in the dark for 1 h. After this, cells were washed 3 × 5 min in 1× PBS again with DAPI (Sigma) added to the last wash at a dilution of 1:10,000 and incubated for 7 min. Coverslips were mounted face down with fluorescent mounting medium (Dako) and dried in the dark for 1 h before visualizing. Images were captured with either a Zeiss LSM710 multiphoton microscope or a Nikon C2 confocal microscope.

Image analysis

Confocal images obtained at 40× objective magnification were used for the analysis of particle intensity of α-synuclein using ImageJ (Fiji, version 1.0), whereas images obtained at 60× objective magnification were used to analyze intensity of autophagy/lysosomal markers (p62, LAMP2, and LC3). The settings were constant for all the images (the scale was set as 4.76 pixels/μm at 40× magnification and 5 pixels/μm at 60× magnification; particles above 2 μm^2 were analyzed). The Threshold tool was used to highlight all stained areas in the field, and the intensity of each particle was measured by the Analyze Particles tool. The Cell Counter plugin allowed cell number to be counted for each image based on DAPI staining. Cells touching the edges of the image and their related particles were excluded from the final analysis. Four to eight images containing 50–100 cells per image were analyzed for each treatment condition. For the analysis of α-synuclein particle size, we defined small particles as 2–5 μm^2, medium particles as 5–10 μm^2, and large particles as >10 μm^2. For spatial analysis of α-synuclein inclusions, 3D images were captured using a Nikon C2 confocal microscope and processed by Huygens Software version 17.10.0.

Crystal violet staining and lactate dehydrogenase release

To assess cell viability and proliferation using crystal violet staining and lactate dehydrogenase release, cells were seeded directly into 12-well plates at a density of 3.5×10^4 cells/well and incubated overnight. The next day, the cells were placed into differentiation media with 5 μg/ml PFF added 4 days after the start of differentiation. The cells were cultured for 12 days longer with the media replaced every 4 days. At the completion of each time point, the cell culture medium was collected and stored at −80 °C, and the cells were washed in 1× PBS and fixed in 4% paraformaldehyde at room temperature for 15 min. At the completion of the entire time course, fixed cells were washed with water and stained with 0.1% crystal violet dye (Sigma) for 20 min. After staining, cells were washed three times with water and air-dried before being shaken with 10% acetic acid at room temperature for 20 min. The extracted samples were then diluted 1:4 in water, and the absorbance at 590 nm was read using a CLARIOstar plate reader. Wells containing no cells were used to determine the background, which was subtracted from the absorbance readings. Lactate dehydrogenase was measured in the stored tissue culture media using the CytoTox96 assay kit (Promega) according to the manufacturer's instructions with the absorbance at 490 nm measured using the CLARIOstar plate reader.

Immunoblot analysis

Cells were lysed in buffer containing 50 mM Tris-HCl, pH 7.5, 1 mM EGTA, 1 mM EDTA, 1 mM sodium orthovanadate, 50 mM sodium fluoride, 5 mM sodium pyrophosphate, 0.27 M sucrose, 1 mM benzamidine, 1 mM phenylmethylsulfonyl fluoride, and 1%

(v/v) Triton X-100. Lysates were clarified by centrifugation at 13,000 × *g* at 4 °C for 20 min, and the supernatant protein concentration was determined by bicinchoninic assay (Thermo Fisher). Up to 30 μg of protein lysates were mixed with sample buffer (2% SDS, 20% glycerol, 2.5% bromphenol blue, 12.5 mM Tris-HCl, pH 6.8, and 5% β-mercaptoethanol) and heated at 70 °C for 10 min before separating by SDS-PAGE. Proteins were then transferred to nitrocellulose membranes followed by blocking in 5% (w/v) skim milk dissolve in 1× TBST (0.87% NaCl, 0.01 M Tris, pH 7.4, and 0.05% Tween 20) for 1 h. The membranes were then cut into strips based on molecular weight markers and incubated in primary antibodies at 4 °C overnight. Horseradish peroxidase–conjugated secondary antibodies were used at room temperature for 2 h. Primary antibodies used for immunoblotting were rabbit monoclonal total ACC (Cell Signaling Technology; 1:1,000), rabbit monoclonal phospho-Ser-79 ACC (Cell Signaling Technology; 1:1,000), rabbit monoclonal total ULK1 (Cell Signaling Technology; 1:1,000), rabbit monoclonal phospho-Ser-555 ULK1 (Cell Signaling Technology; 1:1,000), rabbit monoclonal p70 S6 kinase (Cell Signaling Technology; 1:1,000), rabbit polyclonal phospho-Thr-389 p70 S6 kinase (Cell Signaling Technology; 1:1,000), rabbit monoclonal SQSTM1/p62 (Cell Signaling Technology; 1:1,000), rabbit polyclonal LC3B/MAP1LC3B (Novus; 1:1,000 dilution), rabbit monoclonal phospho-Ser-129 α-synuclein (Abcam; 1:1,000), mouse monoclonal α-synuclein (BD Biosciences; 1:2,000), and β-actin (Abcam; 1:10,000 dilution) as a loading control. Bands were visualized in a Bio-Rad ChemiDoc MP system following enhanced chemiluminescence.

Statistical analysis

Statistical analysis was performed using Prism (GraphPad Software), which was also used to generate graphs. Student's *t* test was used for comparisons between two groups, and one-way ANOVA with Tukey's post hoc test was used for comparisons between multiple groups. Statistical significance was set as $p < 0.05$, and data are presented as mean ± S.D. in the figures.

Author contributions—J. G. formal analysis; J. G., G. P., and M. B. investigation; J. G., G. M. H., and N. D. writing-original draft; G. P. project administration; G. M. H. and N. D. conceptualization; G. M. H. and N. D. supervision; G. M. H. and N. D. funding acquisition; G. M. H. and N. D. methodology; G. M. H. and N. D. writing-review and editing; N. D. data curation.

Acknowledgments—We thank the University of Sydney center for microscopy and microanalysis for access to confocal microscopes and technical assistance. We thank Shikara Keshiya for technical assistance.

References

1. Braak, H., Del Tredici, K., Rüb, U., de Vos, R. A., Jansen Steur, E. N., and Braak, E. (2003) Staging of brain pathology related to sporadic Parkinson's disease. *Neurobiol. Aging* **24,** 197–211 CrossRef Medline
2. Halliday, G., Hely, M., Reid, W., and Morris, J. (2008) The progression of pathology in longitudinally followed patients with Parkinson's disease. *Acta Neuropathol.* **115,** 409–415 CrossRef Medline
3. Olanow, C. W., and Brundin, P. (2013) Parkinson's disease and α synuclein: is Parkinson's disease a prion-like disorder? *Mov. Disord.* **28,** 31–40 CrossRef Medline
4. Steiner, J. A., Quansah, E., and Brundin, P. (2018) The concept of α-synuclein as a prion-like protein: ten years after. *Cell Tissue Res.* **373,** 161–173 CrossRef Medline
5. Kordower, J. H., Chu, Y., Hauser, R. A., Freeman, T. B., and Olanow, C. W. (2008) Lewy body-like pathology in long-term embryonic nigral transplants in Parkinson's disease. *Nat. Med.* **14,** 504–506 CrossRef Medline
6. Li, J. Y., Englund, E., Holton, J. L., Soulet, D., Hagell, P., Lees, A. J., Lashley, T., Quinn, N. P., Rehncrona, S., Björklund, A., Widner, H., Revesz, T., Lindvall, O., and Brundin, P. (2008) Lewy bodies in grafted neurons in subjects with Parkinson's disease suggest host-to-graft disease propagation. *Nat. Med.* **14,** 501–503 CrossRef Medline
7. Luk, K. C., Kehm, V., Carroll, J., Zhang, B., O'Brien, P., Trojanowski, J. Q., and Lee, V. M. (2012) Pathological α-synuclein transmission initiates Parkinson-like neurodegeneration in nontransgenic mice. *Science* **338,** 949–953 CrossRef Medline
8. Desplats, P., Lee, H. J., Bae, E. J., Patrick, C., Rockenstein, E., Crews, L., Spencer, B., Masliah, E., and Lee, S. J. (2009) Inclusion formation and neuronal cell death through neuron-to-neuron transmission of α-synuclein. *Proc. Natl. Acad. Sci. U.S.A.* **106,** 13010–13015 CrossRef Medline
9. Lee, H. J., Suk, J. E., Bae, E. J., Lee, J. H., Paik, S. R., and Lee, S. J. (2008) Assembly-dependent endocytosis and clearance of extracellular α-synuclein. *Int. J. Biochem. Cell Biol.* **40,** 1835–1849 CrossRef Medline
10. Konno, M., Hasegawa, T., Baba, T., Miura, E., Sugeno, N., Kikuchi, A., Fiesel, F. C., Sasaki, T., Aoki, M., Itoyama, Y., and Takeda, A. (2012) Suppression of dynamin GTPase decreases α-synuclein uptake by neuronal and oligodendroglial cells: a potent therapeutic target for synucleinopathy. *Mol. Neurodegener.* **7,** 38 CrossRef Medline
11. Volpicelli-Daley, L. A., Luk, K. C., Patel, T. P., Tanik, S. A., Riddle, D. M., Stieber, A., Meaney, D. F., Trojanowski, J. Q., and Lee, V. M. (2011) Exogenous α-synuclein fibrils induce Lewy body pathology leading to synaptic dysfunction and neuron death. *Neuron* **72,** 57–71 CrossRef Medline
12. Masaracchia, C., Hnida, M., Gerhardt, E., Lopes da Fonseca, T., Villar-Pique, A., Branco, T., Stahlberg, M. A., Dean, C., Fernández, C. O., Milosevic, I., and Outeiro, T. F. (2018) Membrane binding, internalization, and sorting of α-synuclein in the cell. *Acta Neuropathol. Commun.* **6,** 79 CrossRef Medline
13. Mao, X., Ou, M. T., Karuppagounder, S. S., Kam, T. I., Yin, X., Xiong, Y., Ge, P., Umanah, G. E., Brahmachari, S., Shin, J. H., Kang, H. C., Zhang, J., Xu, J., Chen, R., Park, H., *et al.* (2016) Pathological α-synuclein transmission initiated by binding lymphocyte-activation gene 3. *Science* **353,** aah3374 CrossRef Medline
14. Urrea, L., Segura-Feliu, M., Masuda-Suzukake, M., Hervera, A., Pedraz, L., García-Aznar, J. M., Vila, M., Samitier, J., Torrents, E., Ferrer, I., Gavín, R., Hagesawa, M., and Del Río, J. A. (2018) Involvement of cellular prion protein in α-synuclein transport in neurons. *Mol. Neurobiol.* **55,** 1847–1860 CrossRef Medline
15. Cuervo, A. M., Stefanis, L., Fredenburg, R., Lansbury, P. T., and Sulzer, D. (2004) Impaired degradation of mutant α-synuclein by chaperone-mediated autophagy. *Science* **305,** 1292–1295 CrossRef Medline
16. Vogiatzi, T., Xilouri, M., Vekrellis, K., and Stefanis, L. (2008) Wild type α-synuclein is degraded by chaperone-mediated autophagy and macroautophagy in neuronal cells. *J. Biol. Chem.* **283,** 23542–23556 CrossRef Medline
17. Webb, J. L., Ravikumar, B., Atkins, J., Skepper, J. N., and Rubinsztein, D. C. (2003) α-Synuclein is degraded by both autophagy and the proteasome. *J. Biol. Chem.* **278,** 25009–25013 CrossRef Medline
18. Poehler, A. M., Xiang, W., Spitzer, P., May, V. E., Meixner, H., Rockenstein, E., Chutna, O., Outeiro, T. F., Winkler, J., Masliah, E., and Klucken, J. (2014) Autophagy modulates SNCA/α-synuclein release, thereby generating a hostile microenvironment. *Autophagy* **10,** 2171–2192 CrossRef Medline

19. Rideout, H. J., Lang-Rollin, I., and Stefanis, L. (2004) Involvement of macroautophagy in the dissolution of neuronal inclusions. *Int. J. Biochem. Cell Biol.* **36,** 2551–2562 CrossRef Medline
20. Mak, S. K., McCormack, A. L., Manning-Bog, A. B., Cuervo, A. M., and Di Monte, D. A. (2010) Lysosomal degradation of α-synuclein *in vivo*. *J. Biol. Chem.* **285,** 13621–13629 CrossRef Medline
21. Fussi, N., Höllerhage, M., Chakroun, T., Nykänen, N. P., Rösler, T. W., Koeglsperger, T., Wurst, W., Behrends, C., and Höglinger, G. U. (2018) Exosomal secretion of α-synuclein as protective mechanism after upstream blockage of macroautophagy. *Cell Death Dis.* **9,** 757 CrossRef Medline
22. Minakaki, G., Menges, S., Kittel, A., Emmanouilidou, E., Schaeffner, I., Barkovits, K., Bergmann, A., Rockenstein, E., Adame, A., Marxreiter, F., Mollenhauer, B., Galasko, D., Buzás, E. I., Schlötzer-Schrehardt, U., Marcus, K., *et al*. (2018) Autophagy inhibition promotes SNCA/α-synuclein release and transfer via extracellular vesicles with a hybrid autophagosome-exosome-like phenotype. *Autophagy* **14,** 98–119 CrossRef Medline
23. Lee, H. J., Cho, E. D., Lee, K. W., Kim, J. H., Cho, S. G., and Lee, S. J. (2013) Autophagic failure promotes the exocytosis and intercellular transfer of α-synuclein. *Exp. Mol. Med.* **45,** e22 CrossRef Medline
24. Rodriguez, L., Marano, M. M., and Tandon, A. (2018) Import and export of misfolded α-synuclein. *Front. Neurosci.* **12,** 344 CrossRef Medline
25. Alvarez-Erviti, L., Rodriguez-Oroz, M. C., Cooper, J. M., Caballero, C., Ferrer, I., Obeso, J. A., and Schapira, A. H. (2010) Chaperone-mediated autophagy markers in Parkinson disease brains. *Arch. Neurol.* **67,** 1464–1472 CrossRef Medline
26. Murphy, K. E., Gysbers, A. M., Abbott, S. K., Spiro, A. S., Furuta, A., Cooper, A., Garner, B., Kabuta, T., and Halliday, G. M. (2015) Lysosomal-associated membrane protein 2 isoforms are differentially affected in early Parkinson's disease. *Mov. Disord.* **30,** 1639–1647 CrossRef Medline
27. Crews, L., Spencer, B., Desplats, P., Patrick, C., Paulino, A., Rockenstein, E., Hansen, L., Adame, A., Galasko, D., and Masliah, E. (2010) Selective molecular alterations in the autophagy pathway in patients with Lewy body disease and in models of α-synucleinopathy. *PLoS one* **5,** e9313 CrossRef Medline
28. Gan-Or, Z., Dion, P. A., and Rouleau, G. A. (2015) Genetic perspective on the role of the autophagy-lysosome pathway in Parkinson disease. *Autophagy* **11,** 1443–1457 CrossRef Medline
29. Manecka, D. L., Vanderperre, B., Fon, E. A., and Durcan, T. M. (2017) The neuroprotective role of protein quality control in halting the development of α-synuclein pathology. *Front. Mol. Neurosci.* **10,** 311 CrossRef Medline
30. Cerri, S., and Blandini, F. (2019) Role of autophagy in Parkinson's disease. *Curr. Med. Chem.*, in press CrossRef Medline
31. Scrivo, A., Bourdenx, M., Pampliega, O., and Cuervo, A. M. (2018) Selective autophagy as a potential therapeutic target for neurodegenerative disorders. *Lancet Neurol.* **17,** 802–815 CrossRef Medline
32. Campbell, P., Morris, H., and Schapira, A. (2018) Chaperone-mediated autophagy as a therapeutic target for Parkinson disease. *Expert Opin. Ther. Targets* **22,** 823–832 CrossRef Medline
33. Saxton, R. A., and Sabatini, D. M. (2017) mTOR signaling in growth, metabolism, and disease. *Cell* **168,** 960–976 CrossRef Medline
34. Dzamko, N., Gysbers, A., Perera, G., Bahar, A., Shankar, A., Gao, J., Fu, Y., and Halliday, G. M. (2017) Toll-like receptor 2 is increased in neurons in Parkinson's disease brain and may contribute to α-synuclein pathology. *Acta Neuropathol.* **133,** 303–319 CrossRef Medline
35. Curry, D. W., Stutz, B., Andrews, Z. B., and Elsworth, J. D. (2018) Targeting AMPK signaling as a neuroprotective strategy in Parkinson's disease. *J. Parkinsons Dis.* **8,** 161–181 CrossRef Medline
36. Sacino, A. N., Brooks, M. M., Chakrabarty, P., Saha, K., Khoshbouei, H., Golde, T. E., and Giasson, B. I. (2017) Proteolysis of α-synuclein fibrils in the lysosomal pathway limits induction of inclusion pathology. *J. Neurochem.* **140,** 662–678 CrossRef Medline
37. Luna, E., Decker, S. C., Riddle, D. M., Caputo, A., Zhang, B., Cole, T., Caswell, C., Xie, S. X., Lee, V. M. Y., and Luk, K. C. (2018) Differential α-synuclein expression contributes to selective vulnerability of hippocampal neuron subpopulations to fibril-induced toxicity. *Acta Neuropathol.* **135,** 855–875 CrossRef Medline
38. Nonaka, T., Watanabe, S. T., Iwatsubo, T., and Hasegawa, M. (2010) Seeded aggregation and toxicity of α-synuclein and tau: cellular models of neurodegenerative diseases. *J. Biol. Chem.* **285,** 34885–34898 CrossRef Medline
39. Thakur, P., Breger, L. S., Lundblad, M., Wan, O. W., Mattsson, B., Luk, K. C., Lee, V. M. Y., Trojanowski, J. Q., and Björklund, A. (2017) Modeling Parkinson's disease pathology by combination of fibril seeds and α-synuclein overexpression in the rat brain. *Proc. Natl. Acad. Sci. U.S.A.* **114,** E8284–E8293 CrossRef Medline
40. Tanik, S. A., Schultheiss, C. E., Volpicelli-Daley, L. A., Brunden, K. R., and Lee, V. M. (2013) Lewy body-like α-synuclein aggregates resist degradation and impair macroautophagy. *J. Biol. Chem.* **288,** 15194–15210 CrossRef Medline
41. Tarutani, A., Suzuki, G., Shimozawa, A., Nonaka, T., Akiyama, H., Hisanaga, S., and Hasegawa, M. (2016) The effect of fragmented pathogenic α-synuclein seeds on prion-like propagation. *J. Biol. Chem.* **291,** 18675–18688 CrossRef Medline
42. Polinski, N. K., Volpicelli-Daley, L. A., Sortwell, C. E., Luk, K. C., Cremades, N., Gottler, L. M., Froula, J., Duffy, M. F., Lee, V. M. Y., Martinez, T. N., and Dave, K. D. (2018) Best practices for generating and using α-synuclein pre-formed fibrils to model Parkinson's disease in rodents. *J. Parkinsons Dis.* **8,** 303–322 CrossRef Medline
43. Karpowicz, R. J., Jr., Haney, C. M., Mihaila, T. S., Sandler, R. M., Petersson, E. J., and Lee, V. M. (2017) Selective imaging of internalized proteopathic α-synuclein seeds in primary neurons reveals mechanistic insight into transmission of synucleinopathies. *J. Biol. Chem.* **292,** 13482–13497 CrossRef Medline
44. Flavin, W. P., Bousset, L., Green, Z. C., Chu, Y., Skarpathiotis, S., Chaney, M. J., Kordower, J. H., Melki, R., and Campbell, E. M. (2017) Endocytic vesicle rupture is a conserved mechanism of cellular invasion by amyloid proteins. *Acta Neuropathol.* **134,** 629–653 CrossRef Medline
45. Grassi, D., Howard, S., Zhou, M., Diaz-Perez, N., Urban, N. T., Guerrero-Given, D., Kamasawa, N., Volpicelli-Daley, L. A., LoGrasso, P., and Lasmézas, C. I. (2018) Identification of a highly neurotoxic α-synuclein species inducing mitochondrial damage and mitophagy in Parkinson's disease. *Proc. Natl. Acad. Sci. U.S.A.* **115,** E2634–E2643 CrossRef Medline
46. Gitler, A. D., Bevis, B. J., Shorter, J., Strathearn, K. E., Hamamichi, S., Su, L. J., Caldwell, K. A., Caldwell, G. A., Rochet, J. C., McCaffery, J. M., Barlowe, C., and Lindquist, S. (2008) The Parkinson's disease protein α-synuclein disrupts cellular Rab homeostasis. *Proc. Natl. Acad. Sci. U.S.A.* **105,** 145–150 CrossRef Medline
47. Winslow, A. R., Chen, C. W., Corrochano, S., Acevedo-Arozena, A., Gordon, D. E., Peden, A. A., Lichtenberg, M., Menzies, F. M., Ravikumar, B., Imarisio, S., Brown, S., O'Kane, C. J., and Rubinsztein, D. C. (2010) α-Synuclein impairs macroautophagy: implications for Parkinson's disease. *J. Cell Biol.* **190,** 1023–1037 CrossRef Medline
48. Volpicelli-Daley, L. A., Gamble, K. L., Schultheiss, C. E., Riddle, D. M., West, A. B., and Lee, V. M. (2014) Formation of α-synuclein Lewy neurite-like aggregates in axons impedes the transport of distinct endosomes. *Mol. Biol. Cell* **25,** 4010–4023 CrossRef Medline
49. Mazzulli, J. R., Zunke, F., Isacson, O., Studer, L., and Krainc, D. (2016) α-Synuclein-induced lysosomal dysfunction occurs through disruptions in protein trafficking in human midbrain synucleinopathy models. *Proc. Natl. Acad. Sci. U.S.A.* **113,** 1931–1936 CrossRef Medline
50. Alers, S., Löffler, A. S., Wesselborg, S., and Stork, B. (2012) Role of AMPK-mTOR-Ulk1/2 in the regulation of autophagy: cross talk, shortcuts, and feedbacks. *Mol. Cell. Biol.* **32,** 2–11 CrossRef Medline
51. Bobela, W., Nazeeruddin, S., Knott, G., Aebischer, P., and Schneider, B. L. (2017) Modulating the catalytic activity of AMPK has neuroprotective effects against α-synuclein toxicity. *Mol Neurodegener.* **12,** 80 CrossRef Medline
52. Dulovic, M., Jovanovic, M., Xilouri, M., Stefanis, L., Harhaji-Trajkovic, L., Kravic-Stevovic, T., Paunovic, V., Ardah, M. T., El-Agnaf, O. M., Kostic,

V., Markovic, I., and Trajkovic, V. (2014) The protective role of AMP-activated protein kinase in α-synuclein neurotoxicity *in vitro*. *Neurobiol. Dis.* **63,** 1–11 CrossRef Medline

53. Zhang, M., Deng, Y. N., Zhang, J. Y., Liu, J., Li, Y. B., Su, H., and Qu, Q. M. (2018) SIRT3 protects rotenone-induced injury in SH-SY5Y cells by promoting autophagy through the LKB1-AMPK-mTOR pathway. *Aging Dis.* **9,** 273–286 CrossRef Medline
54. Kang, S. S., Zhang, Z., Liu, X., Manfredsson, F. P., He, L., Iuvone, P. M., Cao, X., Sun, Y. E., Jin, L., and Ye, K. (2017) α-Synuclein binds and sequesters PIKE-L into Lewy bodies, triggering dopaminergic cell death via AMPK hyperactivation. *Proc. Natl. Acad. Sci. U.S.A.* **114,** 1183–1188 CrossRef Medline
55. Jiang, P., Gan, M., Ebrahim, A. S., Castanedes-Casey, M., Dickson, D. W., and Yen, S. H. (2013) Adenosine monophosphate-activated protein kinase overactivation leads to accumulation of α-synuclein oligomers and decrease of neurites. *Neurobiol. Aging* **34,** 1504–1515 CrossRef Medline
56. Zhao, Y., Keshiya, S., Atashrazm, F., Gao, J., Ittner, L. M., Alessi, D. R., Halliday, G. M., Fu, Y., and Dzamko, N. (2018) Nigrostriatal pathology with reduced astrocytes in LRRK2 S910/S935 phosphorylation deficient knockin mice. *Neurobiol. Dis.* **120,** 76–87 CrossRef Medline